# Pd/Lewis acid synergy in macroporous Pd@Na-ZSM-5 for enhancing selective conversion of biomass

ChemCatChem

The European Society Journal for Catalysis

Chemistry Europe

European Chemical Societies Publishing

Supported by GECATS GERMAN CATALYSIS SOCIETY

# Accepted Article

**Title:** Pd/Lewis acid synergy in macroporous Pd@Na-ZSM-5 for enhancing selective conversion of biomass

**Authors:** Jia-Wen Liu, Si-Ming Wu, Li-Ying Wang, Ge Tian, Yuan Qin, Jing-Xian Wu, Xiao-Fang Zhao, Yan-Xiang Zhang, Gang-Gang Chang, Lu Wu, Yue-Xing Zhang, Zhao-Fei Li, Cheng-Yu Guo, Christoph Janiak, Silvia Lenaerts, and Xiao-Yu Yang



**To be cited as:** *ChemCatChem* 10.1002/cctc.202000868

**Link to VoR:** https://doi.org/10.1002/cctc.202000868

WILEY-VCH

WILEY-VCH

COMMUNICATION

# Pd/Lewis acid synergy in macroporous Pd@Na-ZSM-5 for enhancing selective conversion of biomass

Jia-Wen Liu,[†[a]] Si-Ming Wu,[†[a, b]] Li-Ying Wang,[†[c]] Ge Tian,[[a]] Yuan Qin,[[a]] Jing-Xian Wu,[[a]] Xiao-Fang Zhao, [[a]] Yan-Xiang Zhang,[[a]] Gang-Gang Chang,[[a]] Lu Wu,[[e]] Yue-Xing Zhang,[[e]] Zhao-Fei Li,[[f]] Cheng-Yu Guo,[[f]] Christoph Janiak,[[g]] Silvia Lenaerts[[h]] and Xiao-Yu Yang*[[a, d ,i]]

[a] J. W. Liu, S. M. Wu, G. Tian, Y. Qin, J. X. Wu, X. F. Zhao, Y. X. Zhang, G. G. Chang, X. Y. Yang
State Key Laboratory of Advanced Technology for Materials Synthesis and Processing & School of Materials Science and Engineering & School of Chemical Engineering and Life Science
Wuhan University of Technology
122 Luoshi Road, Wuhan, 430070, China
E-mail: xyyang@whut.edu.cn

[b] S. M. Wu
Southern Marine Science and Engineering Guangdong Laboratory (Zhuhai) & School of Chemical Engineering and Technology
Sun Yat-sen University (SYSU)
Zhuhai, 519000,China

[c] L. Y. Wang
State Key Laboratory of Magnetic Resonance and Atomic and Molecular Physics
Wuhan Institute of Physics and Mathematics
Chinese Academy of Sciences, Wuhan, 430071

[d] X. Y. Yang
School of Engineering and Applied Sciences
Harvard University
Cambridge, Massachusetts 02138, USA
E-mail: xyyang@seas.harvard.edu

[e] L. Wu, Y. X. Zhang
College of Chemistry and Chemical Engineering
Hubei University
Wuhan, 430062, China

[f] Z. F. Li, C. Y. Guo
Petrochemical Research Institute of PetroChina
Changping District, Beijing, 102206, China

[g] C. Janiak
Institut für Anorganische Chemie und Strukturchemie
Heinrich-Heine-Universität Düsseldorf
40204 Düsseldorf, Germany

[h] S. Lenaerts
Research Group of Sustainable Energy and Air Purification (DuEL), Department of Bioscience Engineering
University of Antwerp
Antwerp, Belgium

[i] X. Y. Yang
Qingdao National Laboratory for Marine Science and Technology
Qingdao, 266237, China

[†]These authors contributed equally to this work.

Supporting information for this article is given via a link at the end of the document.

**Abstract:** Pd nanometal particles encapsulated in macroporous Na-ZSM-5 with only Lewis acid sites have been successfully synthesized by a steam-thermal approach. The synergistic effect of Pd and Lewis acid sites have been investigated for significant enhancement of the catalytic selectivity towards furfural alcohol in furfural hydroconversion.

Nanostructured palladium (Pd) metal, as one of the most efficient catalysts for hydrogenation reactions, has been widely used for biomass conversion.[1-3] However, many issues need to be addressed for the practical application of Pd nanoparticles, such as fast kinetics, high stability, and especially selectivity enhancement.[4-6] Confinement of Pd nanometal in a zeolite matrix is a promising way to a catalyst design that shows significant synergy by combination of well-defined acid sites, shape selectivity, and outstanding stability.[7-10] Zeolite-confined Pd show unique cascade effects on a molecular scale, and thus enables spatially confined catalysis similar to enzyme catalysis.[11-14] The acid sites play a key role in sustainable production of biofuels, such as adsorption promotion of reactants[1,9] and electronically influence of Pd.[15] In the meantime, the confined Pd particles in the acidic zeolite will also strongly influence the state of the acid sites,[16] contributing to the synergy effects of Pd and acid sites. Brønsted acid sites, arising from the framework Al species in highly crystalline zeolites, have been studied for selective conversion.[17-18] However, the strong Brønsted acid sites often lead to the formation of coke and the low stability of Al sites in the zeolite framework, which would decrease the catalyst lifetime.[19] Lewis acidity might circumvent these two problems due to its weaker acidity property and higher stability.[18] It is therefore of

great interests to understand the role of Lewis acid sites in Pd/zeolites catalysts, and thus achieve the high activity, selectivity and stability of Pd/zeolites during selective transformation of renewable biomass-derived feedstocks.[20-22]

However, most studies focus on the Brønsted acid sites in zeolite catalytic systems,[23-25] and there are rare reports on the design and study of Pd/Lewis acid sites. Generally, Brønsted acid sites are attributed to the framework Al in highly crystallized zeolites, which is commonly obtained by hydrothermal process.[26,27] Therefore, to design Pd/Lewis sites system, we present a direct steam-thermal crystallization approach to obtain low crystallized Pd/macroporous ZSM-5 (denoted as Pd@ZSM-5) with a large amount of extra framework Al. For decreasing the number of Brønsted acid sites, $H_3O^+$ ions in ZSM-5 are exchanged by $Na^+$ ions. Macroporosity is introduced in ZSM-5, for increasing the contact of the extra framework Al. The catalysts are then applied in the hydroconversion of furfural (FFL), which is an important and highly unsaturated intermediate in the production of biofuels.[28-31]

Figure 1a illustrates the procedure for the synthesis of Pd@ZSM-5. First $K_2PdCl_4$ was impregnated in mesoporous silica spheres (MS), then $NaAlO_2$ and tetrapropyl ammonium hydroxide solution (TPAOH) were added. The mixture gelated, and was then transferred into an autoclave for steam-assisted crystallization. After calcination in air and reduction under hydrogen atmosphere, Pd@ZSM-5 was obtained (see ESI† for details).

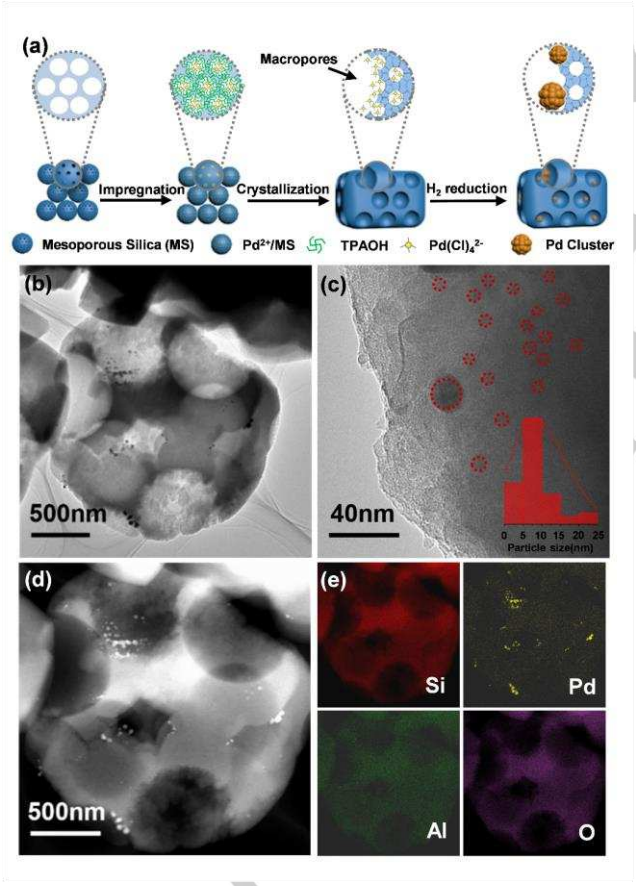


**Figure 1.** (a) Schematic illustration of the synthesis of Pd@ZSM-5. (b), (c) TEM images of Pd@ZSM-5, Inset: The size distribution of Pd nanoparticles in the zeolite. (d) HAADF-STEM image of Pd@ZSM-5 and (e) the corresponding EDX mapping images for Si, Al, Pd, O elements.

SEM and TEM images of Pd@ZSM-5 show 2-3 μm vesicle-like particles, consisting of intergrown primary particles of about 500-700 nm and windows of 500-700 nm (Figure 1, S1 and S2, ESI†). Some of the large Pd particles are obviously in the macropores (Figure 1b, S1 b-d) and some smaller Pd particles can be observed inside the zeolite can be observed inside the zeolite particle with average size of 5-10 nm (Figure 1c). Furthermore, from TEM-EDX element mapping, it can be observed that Pd nanoparticles are dispersed throughout the ZSM-5 particle. XRD patterns match with the MFI structure of ZSM-5 (Figure 2a). The absorption band at 550 $cm^{-1}$ in FT-IR spectra is also associated with the asymmetric stretching mode of the double five-rings in the MFI structure (Figure S3). Notably, no reflections associated with metallic Pd (2theta 40.1°and 46.7°) are observed in the XRD patterns, which is possibly due to the very small particles and the low Pd loading amount (Figure S4). The microporosity of Pd@ZSM-5 was confirmed from $N_2$ adsorption isotherms and the pore size distribution indicates that the formation of Pd nanoparticles does not clearly affect the microporosity (Figure 2b, Table S1).

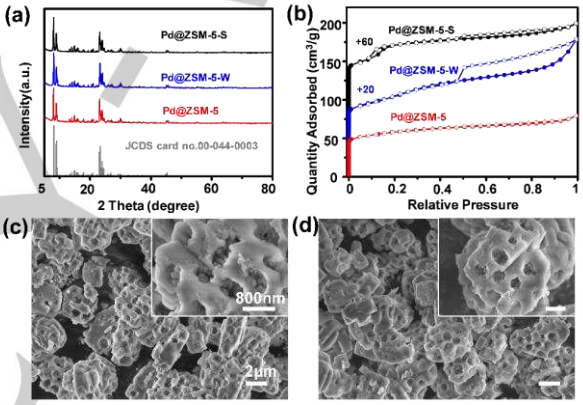


**Figure 2.** (a) XRD patterns of Pd@ZSM-5, Pd@ZSM-5-W and Pd@ZSM-5-S. (b) $N_2$ adsorption/desorption isotherms of Pd@ZSM-5, Pd@ZSM-5-W and Pd@ZSM-5-S; the latter two isotherms are displaced as indicated for clarity. (c) and (d) SEM image of Pd@ZSM-5-W and Pd@ZSM-5-S.

Moreover, the hydrothermal stability and steam stability of Pd@ZSM-5 is assessed by exposing it to water at 110 °C and steam at 110 °C for 3 days (designed as Pd@ZSM-5-W and Pd@ZSM-5-S, respectively). After the thermal treatment, the MFI structure is well-maintained and the microporisity has no obvious change (Figure 2a, b, Table S1). The SEM images (Figure 2c, d) display the well-maintained vesicle-like structure, indicating excellent hydrothermal and steam stability. The EDX analysis in Figure S4 indicates the existence of Al element in Pd@ZSM-5. The signal at 20 ppm in $^{27}Al$ MAS NMR spectrum of Pd@ZSM-5 (Figure S5) shows the presence of large amount of the extra-frame Al sites, indicating the low crystallized structure for the formation of Lewis acid sites. In order to investigate the effect of acidic sites in ZSM-5 zeolite, $Na^+$ ion exchange was applied for decreasing the amount of Brønsted acid sites (designed as Pd@Na-ZSM-5). As comparison, the samples include Pd@H-ZSM-5 (treatment of $NH_4NO_3$ exchange), Pd@S-1 (Silicalite-1 with MFI structure and no any acidic sites using our method), Pd/H-ZSM-5 (macroporous ZSM-5 supported Pd via impregnation-reduction-$NH_4^+$ ion change), Pd/Na-ZSM-5

(macroporous ZSM-5 supported Pd via impregnation-reduction-$Na^+$ ion exchange), Pd/S-1 (macroporous Silicalite-1 supported Pd via impregnation-reduction) (Figure S6) and commercial Pd/C are also obtained.

The unique catalytic properties of zeolite-encapsulated Pd nanoparticles are investigated with the model reaction of hydroconversion of FFL,[6] where various products will form based on the diverse catalytic steps derived by different active sites (Figure 3a).[32] Pd@Na-ZSM-5 shows the highest yield (57%) and selectivity (74%) of furfuryl alcohol (FAL) in comparison with Pd@H-ZSM-5 (14%, 18%) and Pd@S-1 (22%, 30%), Pd/Na-ZSM-5 (7%, 10%), Pd/H-ZSM-5 (16%, 19%), Pd/S-1 (11%, 13%), and commercial Pd/C (13%, 14%) (Figure 3b, Table S2). Compared with the reported catalysts (Table S3), higher selectivity of furfural alcohol is obtained in our work. Note that the by-productions of the catalysts (Pd/Na-ZSM-5, Pd/H-ZSM-5, Pd/S-1, and commercial Pd/C) using impregnation-reduction are considerably high (up to 86%), while the catalysts (Pd@Na-ZSM-5, Pd@H-ZSM-5 and Pd@S-1) using direct transformation show very low amounts of by-products (up to 40% over Pd@S-1). This suggests that the catalysts designed by our synthesis method greatly decreases the by-production and enhances the yield of value-added productions 2-methylfuran (2-MF) and 1,5-pentanediol (PDO) compared with samples obtained by common impregnation method. Very interestingly, only Pd@Na-ZSM-5 show significant selectivity of FAL, which is possibly due to the synergistic effect of Pd and acid sites in Pd@Na-ZSM-5.

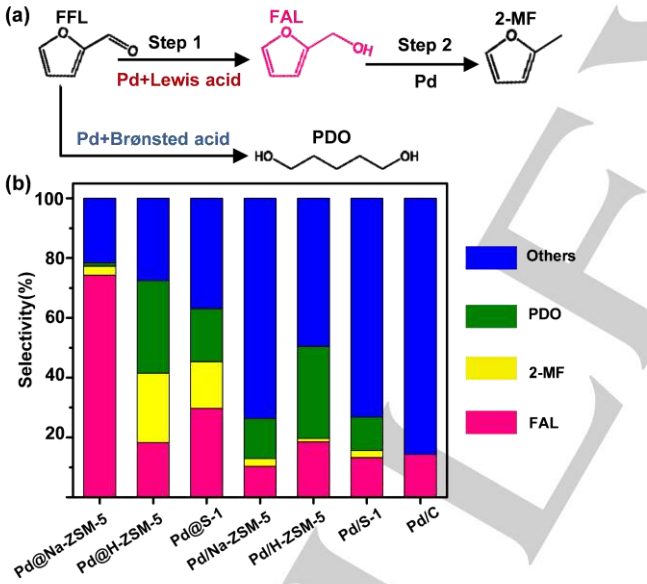


**Figure 3.** (a) Proposed reaction pathways for hydrogenation of furfural. (b) Catalytic performance of furfural hydroconversion over samples. Reaction conditions: 0.03 g of catalyst, 0.8 mmol of furfural, 5 mL of 2-propanol as solvent, 1 MPa $H_2$, T = 150 °C.

The acidic microenvironment of this zeolite might significantly modulate the reaction pathways and product distribution in FFL hydroconversion.[7] Firstly, the acid-base sites provided by the zeolite environment are investigated by $NH_3$ temperature-programed desorption (TPD).[33] The ammonia desorption peak in the temperature range of 50-200°C (1.0 mmol $NH_3$/g) in the $NH_3$-TPD profile of Pd@Na-ZSM-5 (Figure S7) is observed, which is generally assigned to the weak acid sites. As comparison, Pd@H-ZSM-5 show larger amount of weak acid sites (1.8 mmol $NH_3$/g). In the meantime, an additional peak ranging of 300-500 °C of Pd@H-ZSM-5 indicates the existence of strong acid sites in it (0.7 mmol $NH_3$/g). Solid-state NMR is also a very powerful tool for probing the acid sites.[34,35] To further study the Brønsted and Lewis acid sites and to gain insight into the spatial proximity/interaction between the acid sites in ZSM-5, $^1$H magic-angle-spinning (MAS)-NMR and 2D $^1$H double-quantum (DQ) MAS-NMR, both highly sophisticated pulse techniques, have been performed. And to avoid the influence of absorbed water, a pre-dehydration is required before measurement. Figure 4a, b shows the $^1$H MAS NMR spectra of Pd@Na-ZSM-5, Pd/Na-ZSM-5 and Na-ZSM-5 (Figure 4a), and Pd@H-ZSM-5, Pd/H-ZSM-5 and H-ZSM-5 (Figure 4b). Typically, protons residing at Brønsted acid sites, for example, bridging hydroxyls in zeolites, possess $^1$H in range of 3.6-5.6 ppm, whereas weakly acidic terminal hydroxyls, possibly caused by Lewis sites, tend to appear at 1.5-2.0 ppm.[36] It is obvious that all $Na^+$ ion exchanged ZSM-5 (Pd@Na-ZSM-5, Pd/Na-ZSM-5 and Na-ZSM-5) present the sharp and symmetrical

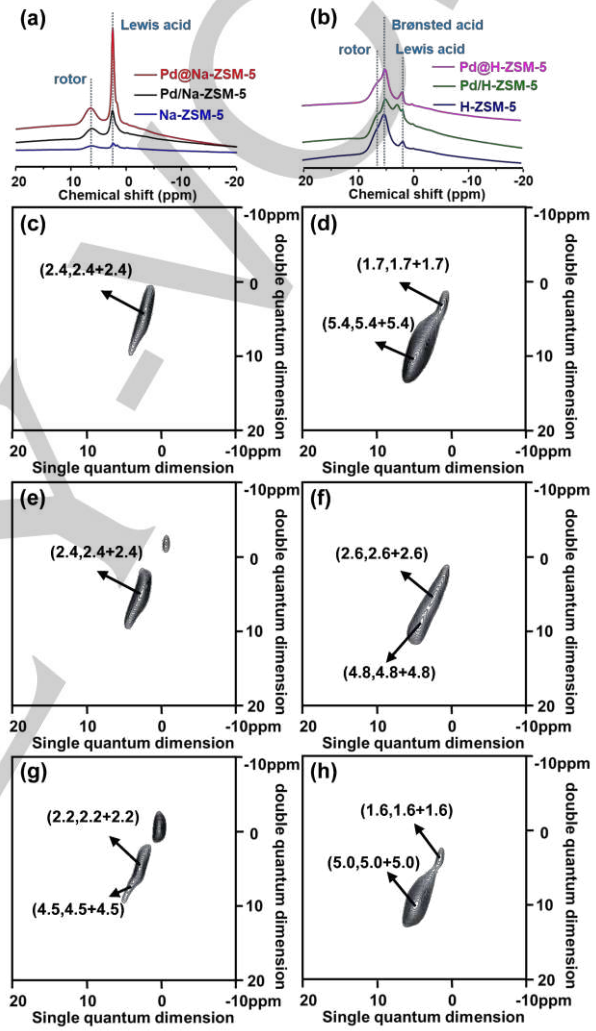


**Figure 4.** (a) $^1$H solid-state MAS NMR spectra of Pd@Na-ZSM-5, Pd/Na-ZSM-5 and Na-ZSM-5, (b) $^1$H solid-state MAS NMR spectra of Pd@H-ZSM-5, Pd/H-ZSM-5, H-ZSM-5. (c)-(h) $^1$H DQ-SQ MAS NMR spectra of (c) Pd@Na-ZSM-5, (d) Pd@H-ZSM-5, (e) Pd/Na-ZSM-5, (f) Pd/H-ZSM-5, (g) Na-ZSM-5 and (h) H-ZSM-5.

signal peak near 2.4 ppm (Figure 4a), indicating the successful control of only Lewis acid sites. Meanwhile, the all H-ZSM-5 based catalysts (Pd@H-ZSM-5, Pd/H-ZSM-5 and H-ZSM-5) show relatively strong signal of Brønsted acid sites at 5.1 ppm and weak signal of Lewis acid sites (Figure 4b).

To further obtain the information about interaction between acid sites of zeolite and Pd, the highly sophisticated pulse technique, 2D $^1$H DQ-SQ MAS NMR, is performed. As shown in Figure 4c, the signal at (2.4, 2.4+2.4) of Pd@Na-ZSM-5 indicates the spatial proximity of hydroxyl groups associated with external framework Al in the supercage, while the strong signal at (5.4, 5.4+5.4) of Pd@H-ZSM-5 (Figure 4d) indicates the main existence of neighboring Brønsted acid sites. Compared with Pd/Na-ZSM-5 and Na-ZSM-5, the $^1$H DQ-SQ MAS NMR spectrum of Pd@Na-ZSM-5 shows only the signal of Lewis acids, suggesting that the direct transformation could create the interaction between the Pd and Lewis acid sites, and the corresponding synergy of Pd and Lewis acid sites leads to significant enhancement of catalytic selectivity.

For further understanding the interaction between the Pd and Brønsted/Lewis acid sites, the X-ray photoelectron spectroscopy (XPS) (Figure 5a) and EPR (Figure 5b) are tested. The two peaks at around 334.5 and 339.9 eV of Pd@Na-ZSM-5 are corresponding to the Pd $3d_{5/2}$ and Pd $3d_{3/2}$ of Pd (0), respectively (Figure S8). Chemical shift of Pd 3d spectra reflects the different states of Pd in each sample. Compared with Pd@S-1, the Pd $3d_{3/2}$ binding energy values of Pd@Na-ZSM-5 and Pd@H-ZSM-5 zeolites shift toward higher values by 0.3 eV and 0.4 eV, respectively (Figure 5a), which is due to the higher electron transfer from palladium to the zeolite framework in the acid environment. Similarly, the stronger signal of the EPR spectra in Pd@Na-ZSM-5 and Pd@H-ZSM-5 (Figure 5b) is also attributed to more active free-electrons than Pd@S-1.[4] Considering the very high hydrogen activation of Pd, the saturation hydrogenation occurs over the Pd@H-ZSM-5, which is in good agreement with the catalytic result (the 2-MF % is higher than the Pd@Na-ZSM-5). The possible mechanism of selective hydrogenation by Pd/Lewis acid and Pd/Brønsted acid models are proposed in Figure 5c. In a Pd/Lewis acid system (Figure 5c, I), the synergistic effect of Pd and Lewis acid sites will promote the adsorption of $H_2$ and the hydrogenation reaction, resulting in the formation of FAL. For Pd/ Brønsted acid system (Figure 5c, II), the protons from bridging hydroxyls in H-ZSM-5 (Si-OH-Al) are more likely to attack the oxygen atoms in furan rings, resulting in the ring opening reaction. Pd that provides excellent hydrogen activation through homolytic $H_2$ cleavage, leads to a saturation hydrogenation and even total hydrogenation to products like PDO. Therefore, different product distributions are obtained in Pd/Lewis acid and Pd/ Brønsted acid system.

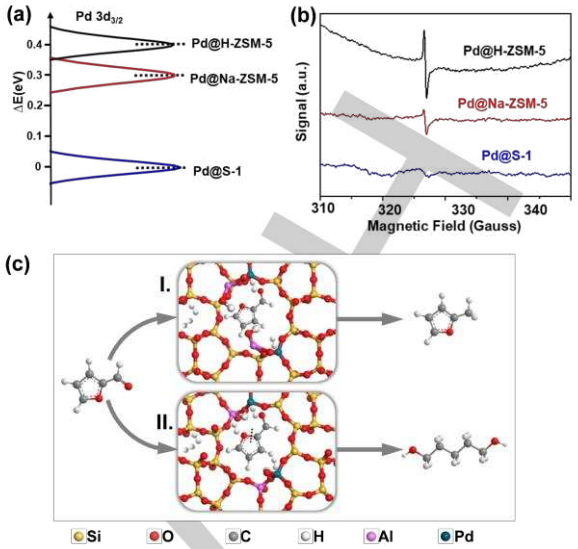


**Figure 5.** (a) Chemical shift of Pd $3d_{3/2}$ XPS spectra of Pd@S-1, Pd@Na-ZSM-5 and Pd@H-ZSM-5. (b) EPR spectra of Pd@S-1, Pd@Na-ZSM-5, Pd@H-ZSM-5 and Pd/C. (c) Schematic illustration of the selective hydrogenation of FFL over the model of (I) Pd/Lewis acid and (II) Pd/Brønsted acid.

In summary, we have successfully designed Pd-encapsulated macroporous ZSM-5 zeolite with high stability. Pd@Na-ZSM-5 shows high selectivity of FAL in the biomass conversion. The interactions between Pd and the acid sites in zeolite has been investigated with multiple techniques and the mechanism of synergistic effect of Lewis acid and Pd is proposed. It is believed that this work provides a new insight for the investigation of highly selective zeolite-encapsulated metal catalysts.

## Acknowledgements

We acknowledge a joint DFG-NSFC project (DFG JA466/39-1, NSFC grant 51861135313). This work was also supported by National Key R&D Program of China (2017YFC1103800), NSFC (U1662134, 21711530705), Jilin Province Science and Technology Development Plan (20180101208JC), HPNSF (2016CFA033), FRFCU (19lgzd16) and ISTCP (2015DFE52870).

**Keywords:** Pd cluster • Lewis acids • confinement effect • synergistic effect • biomass conversion

[1] S. M. Rogers, C. R. A. Catlow, C. E. Chan-Thaw, A. Chutia, N. Jian, R. E. Palmer, M. Perdjon, A. Thetford, N. Dimitratos, A. Villa, P. P. Wells, *ACS Catal.*, **2017**, *7*, 2266-2274

[2] C. Wang, L. Wang, J. Zhang, H. Wang, J. P. Lewis, F. S. Xiao, *J. Am. Chem. Soc.*, **2016**, *138*, 7880-7883

[3] C. Liu, J. Liu, S. Yang, C. Cao, W. Song, *ChemCatChem*, **2016**, *8*, 1279-1282.

[4] A. S. Roy, J. Mondal, B. Banerjee, P. Mondal, A. Bhaumik, Sk. M. Islam, *Appl. Catal. A-Gen.*, **2014**, *469*, 320-327.

[5] Y. X. Xiao., J. Ying., G. Tian, Y. Tao., H. Wei, S. Y. Fan, Z. H. Sun, W. J. Zou, J. Hu, G. G. Chang, X. Y. Yang, *Appl. Catal. B-Environ.*, **2019**, *259*, 118080.

[6] J. Zhang, L. Wang, Y. Shao, Y. Q. Wang, B. C. Gates, F. S. Xiao, *Angew. Chem. Int. Ed.*, **2017**, *56*, 9747-9751.

[7] J. T. Du J. Shi, Q. Sun, D. Wang, H. Wu, J. X. Wang. J. F. Chen., *Chem. Eng. J.*, **2020**, *382*, 122883.
[8] H. J. Cho, D. Kim, J. Li, D. Su, B. Xu, *J. Am. Chem. Soc.*, **2018**, *140*, 13514-13520.
[9] T. L. Cui, W. Y. Ke, W. B. Zhang, H. H. Wang, X. H. Li, J. S. Chen, *Angew. Chem. Int. Ed.*, **2016**, *55*, 9178-9182.
[10] Y. Chai, S. Liu, Z. J. Zhao, J. Gong, W. Dai, G. Wu, N. Guan, L. Li, *ACS Catal.*, **2018**, *8*, 8578-8589.
[11] W. Ke, T. Cui, Q. Yu, M. Wang, L. Lv, H. Wang, Z. Jiang, X. Li, J. Chen, *Nano Res.*, **2017**, *11*, 874-881.
[12] S. M. Wu, X.Y. Yang, C. Janiak, *Angew. Chem. Int. Ed.*, **2019**, *58*, 12340-12354.
[13] M. Limlamthong, A. C. K. Yip, *Bioresource Technol.*, **2020**, *297*, 122488.
[14] N. Wang, Q. M. Sun, J. H. Yu, *Adv. Mater.*, **2019**, *31*, 1803966
[15] X. Y. Yang, L. H. Chen, Y. Li, J. C. Rooke, C. Sanchez, B. L. Su, *Chem. Soc. Rev.*, **2017**, *46*, 481-558.
[16] D. Santi, S. Rabl, V. Calemma, M. Dyballa, M. Hunger, J. Weitkamp, *ChemCatChem*, **2013**, *5*, 1524-1530.
[17] Y. Lou, J. Ma, W. Hu, Q. Dai, L. Wang, W. Zhan, Y. Guo, X.-M. Cao, Y. Guo, P. Hu, G. Lu, *ACS Catal.*, **2016**, *6*, 8127-8139.
[18] S. Telalović, J. F. Ng, R. Maheswari, A. Ramanathan, G. K. Chuah, U. Hanefeld, *Chem. Comm.*, **2008**, *38*, 4631-4633.
[19] S. Xin, Q. Wang, J. Xu, Y. Chu, P. Wang, N. Feng, G. Qi, J. Trébosc, O. Lafon, W. Fan, F. Deng, *Chem. Sci.*, **2019**, *10*, 10159-10169.
[20] I. Yarulina, K. De Wispelaere, S. Bailleul, J. Goetze, M. Radersma, E. Abou-Hamad, I. Vollmer, M. Goesten, B. Mezari, E. J. M. Hensen, J. S. Martinez-Espin, M. Morten, S. Mitchell, J. Perez-Ramirez, U. Olsbye, B. M. Weckhuysen, V. Van Speybroeck, F. Kapteijn, J. Gascon, *Nat. Chem.*, **2018**, *10*, 804-812.
[21] L. Bui, H. Luo, W. R. Gunther, Y. Roman-Leshkov, *Angew. Chem. Int. Ed.*, **2013**, *52*, 8022-8025.
[22] X. Yi, K. Liu, W. Chen, J. Li, S. Xu, C. Li, Y. Xiao, H. Liu, X. Guo, S. B. Liu, A. Zheng, *J. Am. Chem. Soc.*, **2018**, *140*, 10764-10774.
[23] S. H. Pang, J. W. Medlin, *ACS Catal.*, **2011**, *1*, 1272-1283.
[24] J. R. D. Iorio, A. J. Hoffman, C. T. Nimlos, S. Nystrom, D. Hibbitts, R. Gounder, *J. Catal.*, **2019**, *380*, 161-177.
[25] Y. Li, S. Y. Huang, Z. Z. Cheng, K. Cai, L. D. Li, E. Milan, J. Lv, Y. Wang, Q. Sun, X. B. Ma, *Appl. Catal. B-Environ*, **2019**, *256*, 117777.
[26] L. Zhang, L. Chen, Y. Li, Y. Peng, F. Chen, L. Wang, C. Zhang, X.-J Meng, H. He, F.-S. Xiao, *Appl. Catal. B*, **2017**, *219*, 200-208.
[27] T. Y. Ma, H. Li, Q. F. Deng, L. Liu, T. Z. Ren, Z. Y. Yuan, *Chem. Mater.*, **2012**, *24*, 2253-2255.
[28] A. Gualandi, L. Mengozzi, C. M. Wilson, P. G. Cozzi, *Chem. Asian. J.*, **2014**, *9*, 984-995.
[29] Y. Nakagawa, K. Takada, M. Tamura, K. Tomishige, *ACS. Catal.*, **2014**, *4*, 2718-2726.
[30] S. Chen, R. Wojcieszak, F. Dumeignil, E. Marceau, S. Royer, *Chem. Rev.*, **2018**, *118*, 11023-11117.
[31] A. J. Garcia-Olmo, A. Yepez, A. M. Balu, A. A. Romero, Y. W. Li, R. Luque, *Catal. Sci. Technol.*, **2016**, *6*, 4705-4711.
[32] J. Wu, G. G. Chang, Y. Q. Peng, X. C. Ma, S. C. Ke, S. M. Wu, Y. X. Xiao, G. Tian, T. Xia, X. Y. Yang, *Chem. Comm.*, **2020**, *56*, 6297-6300.
[33] R. F. Nie, H. Lei, S. Y. Pan, L. N. Wang, J. H. Fei, Z. Y. Hou, *Fuel*, **2012**, *96*, 419-425.
[34] A. M. Zheng, S. B. Liu, F. Deng, *Chem. Rev.*, **2017**, *117*, 12475-12531.
[35] A. M. Zheng, S. Li, S. B. Liu, F. Deng, *Acc. Chem. Res.*, **2016**, *49*, 655-663.
[36] J. Xu, Q. Wang, F. Deng, *Acc. Chem. Res.*, **2019**, *52*, 2179-2189.

## Entry for the Table of Contents

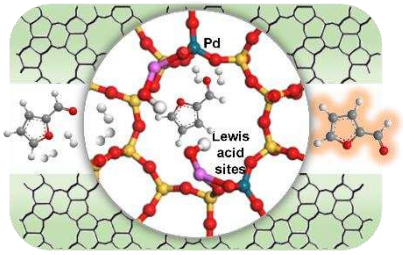


The synergy effect of Pd and Lewis acid sites confined in Pd@macroporous Na-ZSM-5 significantly enhance the catalytic selectivity in biomass conversion.